UDC 551.509.31

ON THE ADJUSTMENT TOWARD BALANCE IN PRIMITIVE EQUATION WEATHER PREDICTION MODELS

HANS ØKLAND

National Meteorological Center,[1] Weather Bureau, ESSA, Washington, D.C.

ABSTRACT

A formal solution of a linear geostrophic adjustment problem for the baroclinic atmosphere is derived. On the basis of this solution, the adjustment toward balance in primitive equation models is discussed with respect to its dependence on scale in space and time, and also with respect to the processes by which the adjustment takes place, that is, the damping and dispersion of the gravitational wave energy. Throughout the discussion, the effect of finite-difference approximations is considered. Finally, a numerical experiment is described that illustrates some of the results from the theoretical investigations.

1. INTRODUCTION

The first discussion of the phenomenon which later has been named geostrophic adjustment is due to Rossby (1938). He considered a straight parallel current of finite width suddenly generated in an unlimited homogeneous ocean, and he showed how the velocity field and the mass field would become adjusted to each other so that a balance between the horizontal pressure force and the Coriolis force was achieved. Cahn (1945) later gave a complete solution of the initial value problem, and Bolin (1953) extended Cahn's solution to a baroclinic ocean. Their solutions consist of a transient part, the inertia-gravitational waves, and a stationary part, a straight current and a pressure gradient in geostrophic balance with each other. The wave energy is allowed to disperse over an infinite domain, so that the amplitude eventually becomes negligible. The solutions were all based on linear perturbation theory. Blumen (1967) and Blumen and Washington (1969) have tried to extend these earlier studies to more general cases.

With the development of primitive equation models for weather prediction, it became important to have initial wind and mass fields that are in balance. How to define and derive this balance has been studied in a number of papers. A thorough study of the problem is given by Phillips (1960). We shall here mention only the fact that if the balance is imperfect, the model will develop inertia-gravitational waves, usually referred to as "noise." It has been demonstrated, however, that the models may gradually develop a better balance during the integration. The balance needed in these models is much more complicated than in the simple linear case just described. Still, there is reason to believe that the mechanism by which the balance is achieved is basically of the same kind.

Proposed methods for obtaining the initial balance involve running the model forward and backward at initial time, utilizing a special numerical device to damp the noise. These methods are strongly related to the adjustment that takes place during a forward integration. Variants of this method involve restoring the mass field (Nitta and Hovermale 1967), and also more complicated manipulations of the nondivergent and the irrotational wind fields (Miyakoda and Moyer 1968).

Using the potential vorticity theorem for a rotating shallow homogeneous fluid, Obukhov (1949) and Washington (1964) find that the height gradients may adjust themselves to the winds, or vice versa, depending on the horizontal scale. Washington introduces what he calls *critical wavelength*, which turns out to be about 15,000 km for middle latitudes. For wavelengths shorter than the critical, the heights are adjusted to the winds.

In this paper, we shall discuss all these points somewhat more in detail, and we shall extend the discussion to a baroclinic atmosphere. For this purpose, we shall derive a formal solution of a perturbation problem similar to those studied by Cahn and Bolin, but without giving any numerical solutions. Although some of the results we shall derive may be looked upon as an extension to the atmosphere of Bolin's study, we shall have our attention mainly directed toward primitive equation models for weather prediction. For this reason, we shall also be discussing the changes to be expected from the introduction of a grid representation in space and time.

2. SOLUTION OF THE LINEAR ADJUSTMENT PROBLEM

The basic flow is assumed to be parallel to the x-axis (not necessarily in the zonal direction), and in geostrophic balance with the geopotential so that $\bar{u}=-f^{1}(\partial\bar{\phi}/\partial y)$, where f, the Coriolis parameter, is assumed to be a constant. Here and later, the bar indicates unperturbated quantities. Pressure, p, is the vertical coordinate. The perturbation, described by the variables u, v, ϕ, and $\omega=dp/dt$ will be assumed to vary with y, p, and t, but not with x. The perturbation equations are

$$(\partial u/\partial t)-fv=0,$$

$$(\partial v/\partial t)+fu+(\partial\phi/\partial y)=0,$$

$$(\partial/\partial t)(\partial\phi/\partial p)+\bar{s}\omega=0,$$

and

$$(\partial v/\partial y)+(\partial\omega/\partial p)=0 \tag{1}$$

where $\bar{s}=-\bar{\alpha}\partial\ln\theta/\partial p$. The boundary conditions on the horizontal boundaries are $(\partial\phi/\partial t)-\bar{\alpha}\omega=0$ for $p=p_0$ (1000 mb) and $\omega=0$ for $p=0$. Here, $\bar{s}$ and $\bar{\alpha}$ are the stability and the specific volume of the unperturbated state.

[1] On leave from the Norwegian Meteorological Institute, Oslo, Norway

Terms like $v\partial\bar{u}/\partial y$, $\omega\partial\bar{u}/\partial p$, $v\partial^2\bar{\phi}/\partial y\partial p$, and $v\partial\bar{\phi}/\partial y$ have been neglected in equations (1) and in the equation for the lower boundary condition. This is justified if the basic flow, $\bar{u}$, is weak at all levels. Similarly, we shall assume that the variation of $\bar{s}$ with y can be neglected so that $\bar{s}$ is a function of p only. With these assumptions, the solution of the perturbation problem is independent of the basic flow.

Assuming that the variation with y and t for all variables is given by the common factor $\exp(iky+i\sigma t)$, where $k=2\pi/L$ and $\sigma=2\pi/T$, the perturbation equations become

$$\begin{aligned} &i\sigma u-fv=0,\\ &i\sigma v+fu+ik\phi=0,\\ &i\sigma(\partial\phi/\partial p)+\bar{s}\omega=0,\\ \text{and}\quad &ikv+(\partial\omega/\partial p)=0, \end{aligned} \tag{2}$$

and the boundary conditions become $i\sigma\phi-\bar{\alpha}\omega=0$ for $p=p_0$ and $\omega=0$ for $p=0$. We assume that all equations in (2) have been divided by $\exp(iky+i\sigma t)$, so that the variables are no longer functions of y and t.

At this point, it is important to note that for $\sigma=0$, the system (2) has the solution $v=\omega=0$ and $u=-ikf^{-1}\phi$ where u and ϕ are functions of p. This solution is seen to be a stationary wind field in geostrophic balance with a geopotential field.

In order to derive the other solutions, we eliminate from (2) all variables but ϕ, and get

$$\frac{\partial}{\partial p}\left(\frac{1}{\bar{s}}\frac{\partial\phi}{\partial p}\right)+\frac{k^2}{\sigma^2-f^2}\phi=0, \tag{3}$$

and the boundary conditions, $(\partial\phi/\partial p)+(\bar{s}/\bar{\alpha})\phi=0$ for $p=p_0$ and $(\partial\phi/\partial p)=0$ for $p=0$.

The last boundary condition (for $p=0$) is the one given by Benwell and Bretherton (1968). It follows from $\omega=0$, assuming that $\bar{s}$ remains bounded as $p\rightarrow 0$. There are different opinions about the correct upper boundary conditions to use (Lindzen et al. 1968). Since we in this paper shall be concerned mainly with weather prediction models, it is sufficient to realize that the vertical structure in these models is described by a finite number of levels, and the differential equation (3), therefore, is substituted by a number of ordinary equations.

In equation (3), the coefficient in front of ϕ has the dimension T^2L^{-2}, and we shall, therefore, write (3) as

$$\frac{\partial}{\partial p}\left(\frac{1}{\bar{s}}\frac{\partial\phi}{\partial p}\right)+\frac{1}{c^2}\phi=0, \tag{4}$$

where

$$c^2=(\sigma^2-f^2)k^{-2}. \tag{5}$$

Inspecting the initial perturbation equations, we realize that c is the phase velocity of a gravity wave on a nonrotating earth. If the values of c can be found from equation (4), the frequency of the inertia-gravitational wave can be derived from (5).

Equation (4) and its boundary conditions are seen to form a Sturm Liouville type boundary value problem (see, for instance, Morse and Feshbach 1953). It defines an infinite number of discrete eigenvalues. We shall call these values c_n^{-2} where $n=1, 2, \ldots$, and where we have assumed that $c_n^{-2}<c_{n+1}^{-2}$. The corresponding solutions of (4), ϕ_n, are known to be orthogonal, in the sense that

$$\int_0^{p_0}\phi_m\phi_n dp=0 \text{ when } m\neq n,$$

and any function of p, F say, may be expressed by a series of the functions ϕ_n in the interval between 0 and p_0:

$$F=\sum^{n}a_n\phi_n$$

where

$$a_n=\int_0^{p_0}\phi_n F dp.$$

It is assumed that the eigenfunctions have been normalized in the sense that

$$\int_0^{p_0}\phi_n^2 dp=1.$$

We shall now construct the formal solution of (1), but first we must decide what the boundary conditions are in the lateral direction. As already mentioned in the introduction, Cahn (1945) and Bolin (1953) gave the solutions for an infinite plane. A similar approach in case of the solution we are considering here would lead to a Fourier integral representation. However, since we are going to concern ourselves mainly with numerical models, a finite domain seems to be more realistic. This would lead to a Fourier series representation of the solution. Models are either solved for the whole globe, in which case the lateral boundary conditions are basically cyclic, or they are solved for a domain bounded by vertical walls where special conditions have to be applied. Since cyclic conditions are simpler for our purpose, they will be used here.

Accordingly, we shall assume that all dependent variables have the same values for y and $y+2D$. The general solution of (1) may then be written

$$\begin{aligned} \phi&=\sum^{k}\left[\hat{\phi}_k+\sum^{n}\phi_n(A_{n,k}\exp(i\sigma_{n,k}t)+B_{n,k}\exp(-i\sigma_{n,k}t))\right]\exp(iky),\\ u&=\sum^{k}\left[-ikf^{-1}\hat{\phi}_k+\sum^{n} ifk^{-1}c_n^{-2}\phi_n(A_{n,k}\exp(i\sigma_{n,k}t)+B_{n,k}\exp(-i\sigma_{n,k}t))\right]\exp(iky),\\ v&=-\sum^{k}\sum^{n}k^{-1}\sigma_{n,k}c_n^{-2}\phi_n(A_{n,k}\exp(i\sigma_{n,k}t)-B_{n,k}\exp(-i\sigma_{n,k}t))\exp(iky),\\ \text{and}&\\ \omega&=-\sum^{k}\sum^{n}i\sigma_{n,k}\bar{s}^{-1}\frac{\partial\phi_n}{\partial p}(A_{n,k}\exp(i\sigma_{n,k}t)-B_{n,k}\exp(-i\sigma_{n,k}t))\exp(iky), \end{aligned} \tag{6}$$

where $\sigma_{n,k}$ is the positive root of (5), $A_{n,k}$ and $B_{n,k}$ are constants, and $\hat{\phi}_k$ is a function of p only. Here, k may have discrete values defined by $k=\pi l D^{-1}$, $l=0, \pm 1, \pm 2, \ldots$. The terms containing $\hat{\phi}_k$ represent the stationary solution mentioned earlier. This solution does not belong to the eigensolutions derived from (4) and must be added separately in order to get the complete general solution of the system (1).

The values of $A_{n,k}$, $B_{n,k}$, and $\hat{\phi}_k$ can be determined from the initial values of ϕ, u, and v. (Since ω at any time may be derived from v, using the equation of continuity, they cannot be prescribed independently.) In order to do so, we make $t=0$ in the solutions, multiply by $\exp(-iky)$, and integrate between the limits $-D$ and D. We then get

$$\phi_k^{(0)}=\hat{\phi}_k+\sum^n (A_{n,k}+B_{n,k})\phi_n,$$

$$u_k^{(0)}=-ikf^{-1}\hat{\phi}_k+\sum^n ifk^{-1}c_n^{-2}(A_{n,k}+B_{n,k})\phi_n,$$

and

$$v_k^{(0)}=-\sum^n \sigma_{n,k}c_n^{-2}k^{-1}(A_{n,k}-B_{n,k})\phi_n \tag{7}$$

where

$$\phi_k^{(0)}=\frac{1}{2D}\int_{-D}^{D}\phi_{t=0}e^{-iky}dy,$$

$$u_k^{(0)}=\frac{1}{2D}\int_{-D}^{D}u_{t=0}e^{-iky}dy,$$

and

$$v_k^{(0)}=\frac{1}{2D}\int_{-D}^{D}v_{t=0}e^{-iky}dy. \tag{8}$$

Here, $\phi_k^{(0)}$, $u_k^{(0)}$, and $v_k^{(0)}$, which are functions of p only, are seen to be the coefficients in the Fourier series expansion of the initial values of the variables.

To proceed, we multiply the equations (7) by ϕ_n and integrate from 0 to p_0;

$$\int_0^{p_0}\phi_k^{(0)}\phi_n dp=\int_0^{p_0}\hat{\phi}_k\phi_n dp+A_{n,k}+B_{n,k},$$

$$\int_0^{p_0}u_k^{(0)}\phi_n dp=-ikf^{-1}\int_0^{p_0}\hat{\phi}_k\phi_n dp+ifk^{-1}c_n^{-2}(A_{n,k}+B_{n,k}),$$

and

$$\int_0^{p_0}v_k^{(0)}\phi_n dp=-\sigma_{n,k}k^{-1}c_n^{-2}(A_{n,k}-B_{n,k}).$$

Solving for $A_{n,k}$, $B_{n,k}$, and $\hat{\phi}_k$, we finally get

$$\frac{ik}{f}\int_0^{p_0}\hat{\phi}_k\phi_n dp=\frac{ik}{f}\frac{f^2}{\sigma_{n,k}^2}\int_0^{p_0}\phi^{(0)}\phi_n dp-\left(1-\frac{f^2}{\sigma_{n,k}^2}\right)\int_0^{p_0}u^{(0)}\phi_n dp, \tag{9}$$

$$A_{n,k}=\frac{1}{2}\left(1-\frac{f^2}{\sigma_{n,k}^2}\right)\left[\int_0^{p_0}\phi^{(0)}\phi_n dp-\frac{if}{k}\int_0^{p_0}u^{(0)}\phi_n dp\right]-\frac{kc_n^2}{2\sigma_{n,k}}\int_0^{p_0}v^{(0)}\phi_n dp, \tag{10}$$

and

$$B_{n,k}=-\frac{1}{2}\left(1-\frac{f^2}{\sigma_{n,k}^2}\right)\left[\int_0^{p_0}\phi^{(0)}\phi_n dp-\frac{if}{k}\int_0^{p_0}u^{(0)}\phi_n dp\right]+\frac{kc_n^2}{2\sigma_{n,k}}\int_0^{p_0}v^{(0)}\phi_n dp. \tag{11}$$

The integral on the left-hand side of (9) is seen to be the coefficient in an expansion of $\hat{\phi}_k$ in terms of the functions ϕ_n. Therefore, (6) together with (9), (10), and (11) represent our solution of the initial value problem. A basically similar solution has been used by Ogura and Charney (1962) in their discussion of a mesoscale model.

3. SOLUTION FOR FINITE DIFFERENCES

Before proceeding to a general discussion of the solution just given, we shall see what changes a grid-point representation of the variables may cause in the solution. As already mentioned in connection with the upper boundary condition, a grid-point representation in the vertical coordinate gives a set of ordinary homogeneous equations to solve, instead of the differential equation (3). The number of eigenvalues will be limited and, in general, corresponds to the number of grid points (levels). To each eigenvalue corresponds a set of grid-point values, the eigensolution.

There are numerous widely different modeling techniques in use for the vertical structure of weather prediction models. However, we do not want to tie our discussion to a particular model, and we shall, therefore, consider only the continuous vertical solution described by the eigenfunctions ϕ_n, since many of the properties of these functions can be expected also of the eigensolutions for a discrete model. We shall mention some of these properties which are of importance for our discussion, but we refer the reader to Morse and Feshbach's book (1953) for the proofs. First, the eigenvalues are all positive if $\bar{s}>0$ for all values of p. Second, the eigenfunctions, ϕ_n, will change sign $n-1$ times as p increases from 0 to p_0. Therefore, when a function is expanded in a series of ϕ_n, the first term will give mostly the mean vertical character, while the other terms will give more and more of the details as n increases.

Concerning the effect of a horizontal grid-point representation, we shall be more specific, since we shall assume that all variables are given in the same grid points and that the derivatives are approximated by centered differences. Other schemes are in use, but most of them have basically the same effect on the solution as the one discussed here. Since the variation in the horizontal direction has been expressed by a Fourier series, we need only study the effect of the finite-difference approximation on one harmonic component, say e^{iky}. For the first space derivative, we get $(\partial/\partial y)e^{iky}\approx ik'e^{iky}$ where

$$k'=(\Delta y)^{-1}\sin(k\Delta y), \tag{13}$$

and we can obviously get the solutions for the finite-difference case by changing k to k' in equations (2) to (11).

Next we shall consider the effect of finite differences in time. It is readily understood that a centered time step could be treated in the same way as the centered space difference, since we have assumed a harmonic time variation for each component of the solution. Therefore, we can simply substitute σ by $(\Delta t)^{-1}\sin(\sigma'\Delta t)$ in equations (2) to (5), and from (5) we then get

$$\sigma' = (\Delta t)^{-1} \arcsin[(f^2+k^2c^2)^{1/2}\Delta t], \tag{14}$$

where we only use the value in the first quadrant, thus disregarding the so-called computational mode (Kurihara 1965). In the final solutions (6), (9), (10), and (11), the exponential functions will be changed to $\exp(\pm i\sigma'_{n,k}\,\tau\Delta t)$, while $\sigma_{n,k}$ elsewhere has the value given by (5). Here, τ is the number of time steps. Thus, the time-dependent part of the solution will consist of waves with no damping of the amplitude, just as in the continuous case, but the speed of propagation will be different. The usual linear stability criterion is tied to equation (14), which gives real values of σ' only if $(f^2+k^2c^2)^{1/2}\Delta t<1$.

As already mentioned, selective damping of the high frequencies may deliberately be introduced in numerical models by certain types of time-difference schemes. One such scheme is the "Euler-backward," which recently has become very popular (Kurihara 1965). We shall, therefore, investigate also the effect of this scheme on the solution.

The Euler-backward time step consists of one preliminary forward step, which thereafter is substituted by an adjusted step. Assuming that the time variation is harmonic or exponential, a forward step would change all variables by a factor r^*, where r^* in general is complex. Similarly, the following adjusted step would change the variables by a factor r. Introducing this in (1), we get for the adjusted step

$$\frac{r-1}{\Delta t}u-r^*fv=0,$$

$$\frac{r-1}{\Delta t}v+r^*fu+ir^*k\phi=0,$$

$$\frac{r-1}{\Delta t}\frac{d\phi}{dp}+r^*\bar{s}\omega=0,$$

and

$$ir^*kv+r^*\frac{d\omega}{dp}=0, \tag{15}$$

and for the boundary conditions $(r-1/\Delta t)\phi-r^*\bar{\alpha}\omega=0$ for $p=p_0$ and $r^*\omega=0$ for $p=0$. Dividing these equations by r^* we get the same form as in (2), and by elimination of all the variables but ϕ, we derive essentially the same boundary value problem as (4), but (5) is substituted by

$$\left(\frac{r-1}{r^*\Delta t}\right)^2=-f^2-k^2c^2. \tag{16}$$

A similar set of equations defining the preliminary forward step may be derived from (1) simply by substituting $(r^*-1)\Delta t^{-1}$ for $i\sigma$ in (2), and from these equations we get

$$\left(\frac{r^*-1}{\Delta t}\right)^2=-f^2-k^2c^2. \tag{17}$$

Elimination of r^* gives

$$r=1\pm i\Delta t(k^2c^2+f^2)^{1/2}-(\Delta t)^2(k^2c^2+f^2).$$

This formula is similar to the one derived by Kurihara (1965) for the barotropic atmosphere.

Writing $r=R\exp(i\sigma'\Delta t)$, we get

$$R^2=1-(\Delta t)^2(k^2c^2+f^2)+(\Delta t)^4(k^2c^2+f^2)^2. \tag{18}$$

R is the damping factor associated with one time-step, provided the stability criterion is fulfilled. Similarly, we get for the new frequency

$$\sigma'=(\Delta t)^{-1}\arctan\left(\frac{\Delta t(k^2c^2+f^2)^{1/2}}{1-(\Delta t)^2(k^2c^2+f^2)}\right). \tag{19}$$

Since in this case (15) takes the place of (2), we obviously can derive the complete solution from the expressions (6) to (11) by changing the exponential function to $R^{\tau}_{n,k}\exp(\pm i\sigma'_{n,k}\tau\Delta t)$, where $R_{n,k}$ and $\sigma'_{n,k}$ are derived from (18) and (19), using the appropriate values of c_n and k.

4. ADJUSTMENT TOWARD BALANCE IN NUMERICAL MODELS

The assumptions underlying the problem just considered—a weak basic flow, perturbation independent of x, etc.—are rather special, and we would not generally expect them to be true in the real atmosphere or in a numerical weather prediction model. Instead, we must consider a balance between wind and mass field which is much more complicated than the geostrophic equilibrium we have considered: the fields are strong and curved, and generally transient; the balanced wind field is no longer nondivergent, but contains a small but significant irrotational part (Phillips 1960). Nevertheless, we feel justified in assuming that an adjustment takes place in a manner very similar to the one considered earlier in this paper. More specifically, we believe that the solution to the general initial value problem analogous to (6), if it could be derived, would consist of two parts, the one being the inertia-gravitational waves with high frequencies and the other the balanced mass and wind fields which also are transient, but with much lower frequency. A crucial point is whether the dependence on scale and latitude which we find in our solution takes place also in the general case. We shall assume that this is true at least to some extent, and we shall later describe some experiments that support this assumption.

In Cahn's (1945) and Bolin's (1953) solutions, the wave energy could disperse over an infinite domain. This is no longer the case with the solution we consider, since we have assumed a finite domain. Energy may very well disperse from a source area, and this will bring the fields in the source area closer to the balance. However, the total wave energy integrated over the whole domain will be conserved as long as we consider the continuous solution, and also the finite-difference solution with the centered time step. The Euler-backward scheme, however, gradually reduces the transient part of the solution, and we are finally left with the stationary part.

In the following, we shall first discuss some properties of the adjusted state in relation to the initial perturbation. Later, we shall return to the adjustment process itself and try to draw some useful conclusions concerning weather prediction models.

5. RELATION BETWEEN THE INITIAL DISTURBANCES AND THE NEW BALANCE

The left-side of equation (9), multiplied by $\phi_n e^{iky}$, is the adjusted geostrophic wind field for a component characterized by the vertical scale number n and the horizontal angular wave number k. The right-hand side of (9) shows that this new balance does not depend on the initial value of v. The analogy to v in the general case would be the irrotational part of the wind, and we are, therefore, led to the conclusion that if the nondivergent wind is in balance with the mass field, a false or missing irrotational wind would give rise to inertia-gravitational waves. However, if the wave energy is dispersed or damped, we would presumably be left with an irrotational wind field appropriate to the balance, while the nondivergent wind field and the mass field are unchanged.

Returning to the right-hand side of equation (9), we observe that the ratio between f and $\sigma_{n,k}$ determines which term is of most importance. If $\sigma_{n,k} \gg f$, the adjusted geopotential corresponds closely to the initial wind through geostrophic wind relation, while the initial geopotential is of little importance. In the opposite case when $\sigma_{n,k} \approx f$, the geopotential undergoes small changes, while the wind adjusts itself to the geopotential. Here $\sigma_{n,k}$ depends on the horizontal and vertical scale of the perturbation, and also on the static stability, while f depends on the latitude. We may state as a general rule that height will tend to be adjusted to the wind for small horizontal scales and large vertical scales, and more so in low latitudes. The dependence on static stability is more complicated, but since c_n tends to increase when the stability increases, the general rule is that high stability acts in the direction of adjusting the mass to the wind field. The considerations in this paragraph are in agreement with the results derived by Fjørtoft. (1951).

Washington's *critical wavelength* (1964) corresponds to the case when $\sigma^2_{n,k}=2f^2$. Benwell and Bretherton (1968) computed the values of c_n for a 10-level model and found 286, 111, 43.5, 26, and 16 m sec^{-1} for the first five modes. From these values, we derive the critical wavelengths 18 $\times 10^6$, 7×10^6, 2.7×10^6, 1.6×10^6, and 1.0×10^6 m, respectively (for $f=10^{-4}$ sec^{-1}). For a two-level model, we have found $c_1=297$ m sec^{-1} and $c_2=42$ m sec^{-1}, which gives 18.7×10^6 m and 2.6×10^6 m, respectively. The value corresponding to the first mode, the so-called external gravity mode, is close to the value given by Washington (1964) for the homogeneous case.

Introducing finite differences in time will not change the considerations above, since the change would be only in the transient part of the solution. Space differences, however, will have a significant influence on the smaller scales in the horizontal dimension. Since $\sigma^2_{n,k}$, which occurs explicitly in (9), now has the value $(f^2+k'^2c_n^2)$, we can discuss the effect of finite differences by comparing the magnitude of k and k'. These two quantities are tabulated in table 1. From this table we can see, for instance, that with a grid representation, a wave component three increments long will behave like a component more than seven increments long in case of continuous functions.

TABLE 1.—*The $k=2\pi/L$ and $k'=\Delta y^{-1}$ sin $(k\Delta y)$ for different wavelengths, L.*

$L/\Delta y$	2.0	2.5	3.0	3.5	4	5	6	7	8	10
$k\Delta y$	3.14	2.51	2.09	1.79	1.57	1.26	1.05	0.90	0.79	0.63
$k'\Delta y$	0	0.59	0.87	0.97	1.00	0.95	0.87	0.78	0.71	0.59

Therefore, there will be a tendency for the shortest components to behave like the longest, in the sense that the wind will tend to adjust itself to the geopotential. It should also be noted that because k' is much less than k for the shortest components, the wind computed geostrophically from the height becomes too weak. The combined effect on the shortest components is then seen to be that there will be little change in the geopotential, while the wind becomes weak.

In the discussion above, we have treated k as a continuous variable. It should be borne in mind that it actually will take on only discrete values in a finite domain, and indeed a finite number of different values if a grid representation is considered.

6. SUPPRESSION OF THE INERTIA-GRAVITATIONAL WAVES

It was mentioned that a numerical model can approximate a balanced state by dispersion of wave energy from a source area and/or by damping of the high-frequency oscillations. We shall now first discuss some aspects of the damping procedure, while the dispersion will be treated in the next section.

The Euler-backward integration scheme was introduced earlier in this paper as a means to get an artificial damping of the time-dependent part of (6), and it was shown that the amplitudes of the waves were reduced by a factor R for each time step, where R is given by equation (18).

Obviously, the damping depends on the frequency of the oscillation. The length of the time step, Δt, has to be so short that the component with the highest frequency is computationally stable, which means that $(f^2+k^2c_n^2)(\Delta t)^2$ is much less than 1 for most of the components. Therefore, according to equation (18), the rate of damping of a particular component is approximately proportional to the square of the frequency. This property of the damping becomes very important when general dynamic models of the atmosphere are considered, since then also the balanced state is transient, but with a relatively low frequency. As an example, let us take the two-level model referred to earlier. With $L=3500$ km and $f=10^{-4}$ sec^{-1}, we get $\sigma^2=29.4\times 10^{-8}$ sec^{-2} for the external mode, and 1.57×10^{-8} sec^{-2} for the internal, which shows that the external mode is damped nearly 20 times faster than the internal. Actually, since the period for the higher vertical modes approaches the period for the inertia wave (half a pendulum day), we will not have a good separation between the frequency of these modes and the frequency of the balanced state. Therefore, one cannot expect to obtain a good balance for a multilevel model in this way without also damping the fields one wants to retain.

Space differencing in the y-direction will lead to lower frequency for the short wavelengths as already shown in section 3. Indeed, the wavelength $2\Delta y$ will have the pure inertial frequency. Therefore, the shortest scales will be adjusted only slowly to a balance by the damping device we have been discussing.

Nitta and Hovermale (1967) showed that one forward time-step followed by one backward, using the Euler-backward scheme, brings the phase back to its initial value, while the amplitude of the waves is reduced by a factor R^2. This result is easily derived from the solution we have given earlier for the Euler-backward scheme. Obviously, this is a simple method of improving the initial balance. The adjusted geostrophic balance will have the same dependence of the initial fields as we have discussed earlier. Also, the rate at which the adjustment takes place will have the same relation to the frequency as we have just found for the forward time integration.

Some of the results we have deduced from the linear analyses are supported by experiments described by Dey (1969). Using a barotropic primitive equation model, and the 500-mb height and wind analyses, he ran forecasts up to 36 hr both with the centered time step and the Euler-backward. The former scheme produced a rough and "wiggly" forecast compared to the latter, obviously because of inertia-gravitational waves introduced by poor initial balance. It could be shown, however, that in both cases the height was adjusted to the wind for the large-scale feature. The same also occurred when running the model back and forth, using a damping finite-difference scheme. Similar experiments have been reported by Nitta (1968).

7. DISPERSION OF WAVE ENERGY

In case of a continuous spectrum, the propagation of wave energy takes place with the group velocity, defined by

$$c_{gr}=\partial(k\,c_{ph})/\partial k \tag{20}$$

where c_{ph} is the phase velocity. In our case, the spectrum is not continuous, and the above formula should be expressed in terms of differences instead of differentials. However, this would make little difference if we consider waves that are considerably smaller than the dimension of the domain, and we shall, therefore, use the above formula, since it is simpler for our purpose.

The pure gravitational waves are nondispersive, since the phase velocity does not depend on the wave number. However, the combined inertia-gravitational waves are dispersive, a fact which has been pointed out also by Washington (1964) and others. Of considerable interest from our point of view is that in case of a grid-point representation also the pure gravitational wave is dispersive. In the following, we shall try to show what significance this might have for numerical models.

TABLE 2.—*Reduction in group velocity when space differences are used*

$L/\Delta y$	2	2.5	3	3.5	4	5	6	7	8	10
K	0	−0.19	−0.21	−0.12	0	0.23	0.41	0.54	0.64	0.76

From equations (5) and (20), we easily derive a formula for the group velocity, which for our purpose may be written conveniently as

$$c_{gr}=c_n(c_n/c_{ph}) \tag{21}$$

where

$$c_{ph}=(c_n^2+f^2/k^2)^{1/2}. \tag{22}$$

This shows that if c_n is large, which especially is the case for the external mode, c_{gr} is approximately equal to c_n and, therefore, also large. If c_n is small, the group velocity is still smaller, especially for long waves in high and middle latitudes.

If space differences are taken into account, the formula for the group velocity given in equation (21) will contain also a factor $K=\sin(2k\Delta y)/2k\Delta y$, and in the equation (22) k must be changed to k'. Some values of K are given in table 2. Obviously, the group velocity for the shorter waves is greatly reduced where a grid representation is applied. The circumstance that K becomes negative for wavelengths between $2\Delta y$ and $4\Delta y$ is of no special importance here, since there are two waves which move in opposite directions.

If time differences are also taken into account, one gets still another factor on the right-hand side of equation (21). In case of the centered time step, this factor turns out to be $(1+(c_{ph}\Delta t)^2)^{-1/2}$ and for the Euler-backward time step $(1+(c_{ph}\Delta t)^2)\cdot(1-(c_{ph}\Delta t)^2+(c_{ph}\Delta t)^4)^{-1}$. For most wave components, $c_{ph}\Delta t \ll 1$; and, therefore, the time differencing will change the group velocity very little.

An implication for weather prediction models is that if the initial data in a limited horizontal area gives rise to waves with small group velocity, the wave energy will disperse slowly, and the adjustment accordingly will be slow. We shall have the opportunity to return to this point in the next section.

8. A NUMERICAL EXPERIMENT

In this last section, we shall describe an experiment illustrating some of the conclusions in the previous sections. A two-level primitive equation model was used, and initial data were operationally analyzed winds and heights for the 300- and 700-mb surface and sea-level pressure. Using the Euler-backward scheme, a 24-hr forecast was computed. At that time, the noise introduced initially by poorly balanced data had been damped, and the model seemed to be in a fairly good state of balance. This prognosis was then used as initial data for two new 24-hr

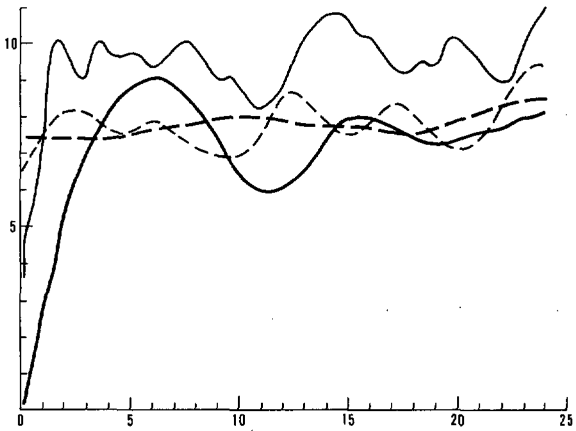

FIGURE 1.—RMS of ω (heavy lines) and of sea-level pressure tendencies (thin lines) for two forecasts, one (continuous lines) without initial divergence, the other (broken lines) with initial divergence. Units on the abscissa are hours forecast time, on the ordinate 10^{-4} mb/sec for ω and 2×10^{-2} mb/10 min for the pressure tendencies.

integrations. In the one case, the data were used without changes; in the other case, the irrotational part of the wind was removed. In both cases, the centered time step was applied.

The graphs in figure 1 show the time change in the RMS (root mean square) of ω (heavy lines) and the RMS of the surface pressure tendencies (thin lines). The broken lines correspond to the case with the divergence included initially. The RMS was computed at each time step from the values in the interior grid points of the entire domain. Obviously, the integration with nondivergent initial values is less in balance than the other, measured by the general level of high-frequency noise. This is particularly true of the pressure tendencies, where the mean value is considerably higher in the nondivergent case. The oscillations that show up in the graphs must be caused by some dominant scale with a characteristic frequency.

The model, which has been referred to earlier, is capable of producing two vertical modes, the external and the first internal ones. From the solution (6) for ω and the general properties of the eigenfunctions, ϕ_n, it is easily concluded that for a characteristic value of the mass perturbation, the higher vertical modes have comparatively larger values of the vertical velocity associated with them. For this reason, the graphs of ω show mostly the effect of the internal mode, while the external mode shows up more clearly in the surface pressure tendencies.

In figure 1, we observe that the nondivergent case shows an oscillation of large amplitude around a mean value which is close to the mean value for the divergent case. It takes the model close to 12 hr to reach the first minimum, and if we take this to be the characteristic period, we can compute a characteristic wavelength from a formula similar to (5):

$$4\pi^2T^{-2}=f^2+4\pi^2(L_x^{-2}+L_y^{-2})c^2$$

where L_x and L_y are the wavelengths in the x- and y-directions, respectively, T the period, and c the speed of the pure gravitational wave. For the model used, c has been computed by linear analyses to be 297 m sec^{-1} and 42 m sec^{-1} for the external and the internal modes, respectively (using values from the U.S. Standard Atmosphere). Assuming that the oscillation just mentioned is the internal mode, that $L_x=L_y$, and that $f=10^{-4}$ sec^{-1}, one gets $L=3500$ km.

Comparing the two graphs for the sea-level pressure tendencies, we see that we here have introduced oscillations of much shorter period by removing the divergence initially. It must be noted, however, that the pressure tendencies associated with a certain wave component oscillates around zero as the equilibrium value, while ω oscillates around a nonzero value (this will become evident later when we discuss the actual ω fields). For this reason, the RMS of the pressure tendencies more likely will show two maxima and two minima during a period. An inspection of the curve and also the pressure variations in a number of grid points show a characteristic period of about 3 hr for this rapid oscillation. Assuming that this is the external mode, we get $L = 4500$ km. This is a somewhat larger value than the one derived above. However, the solutions for ω and ϕ in equations (6) show that a shorter horizontal scale has comparatively larger values of the vertical velocity associated with it, since $\sigma_{n,k}$ is larger, and that, therefore, a smaller scale will dominate in the RMS of ω, other conditions being equal.

We therefore feel justified to assume that it is the same horizontal scales which have been excited in both cases. We may also note that this is a typical scale for the extratropical cyclones. The oscillations must have been started because the irrotational wind field, which is a necessary part of the balance, is removed. Furthermore, since the divergence in the balanced state is tied to the nondivergent wind field, we must expect the oscillation to have the same scale as the nondivergent wind.

It may be interesting to see how well the oscillations in ω, which we have described, show up also on the maps of the prognostic fields. A section of such maps is shown in figures 2A to 2D, where lines are drawn for ω and 700-mb contours. Figure 2A shows the ω field derived from the irrotational wind field removed initially, and 2B, 2C, and 2D, the 6-, 12-, and 18-hr forecasts. The vertical velocity, being zero initially, increases to comparatively large values at 6 hr, decreases again to very small values, and then increases again. Apart from this oscillation, the areas with upward and downward motion change very slowly with time. This must be attributed to the rather small group velocity for this scale—only 18 m sec^{-1} according to the formulas derived earlier. Of course, eventually the wave energy will disperse.

It may also be mentioned that as far as the nondivergent part of the wind is concerned, there are no significant differences between the two forecasts. This is in agreement

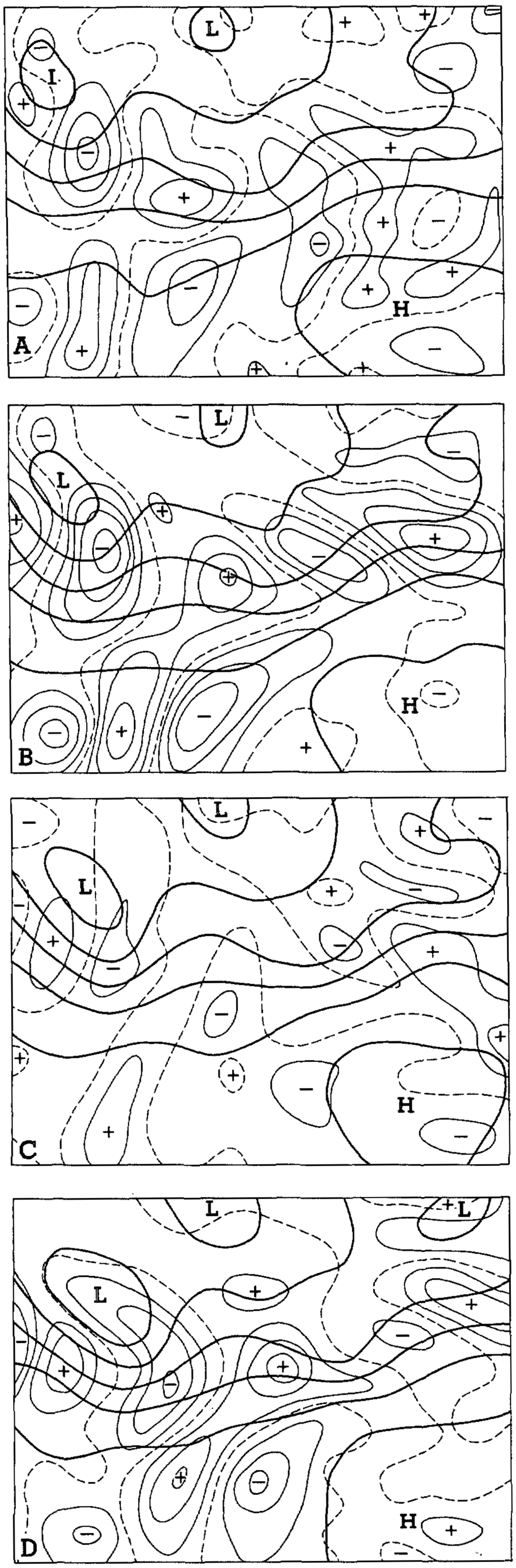

FIGURE 2.—(A) vertical velocity (ω) and 700-mb contours initially and for (B) the 6-, (C) 12-, and (D) 18-hr forecasts. The initial divergence was removed from the wind fields before the start of the forecast.

with the results derived in section 5 about the effect of the irrotational wind on the final adjusted state.

9. CONCLUDING REMARKS

The discussion in this paper has centered around a simple linear model of the atmosphere. For this model, we have been able to derive a solution to the problem of how the model adjusts itself to a balanced state. Some aspects of this solution are assumed to be generally true for primitive equation prediction models; for instance, the final balanced state can be determined from the initial values of the variables, and the difference between this balanced state and the initial values may be expressed as a series of inertia-gravitational wave components, corresponding to the free modes of oscillation in the model. If the model shall approach the balanced state, it is necessary that these waves are dispersed, dissipated, and/or damped by some other means. As we have seen the damping brought about by the device we have focused the attention on, the Euler-backward integration scheme affects mostly the highest frequencies, which are chiefly associated with the external gravitational model. A barotropic primitive equation model has only one gravitational mode, with a frequency comparable to the external mode in baroclinic models, and consequently a rapid adjustment toward the balance. In a barotropic model, this is also the case for the part of the initial unbalance which can be expressed in terms of the first vertical mode in the expansion we have used. The higher vertical modes, however, are adjusted rather slowly to a balanced state. Furthermore, since the group velocity is small for these modes, the wave energy disperses only slowly. As we have seen, this is especially crucial for the vertical velocity, and therefore for the simulation of the condensation processes.

As we stated above, the new balance depends on the initial values of the variables. In the barotropic model, the balance is mostly determined by the initial wind. Again, in a baroclinic model, we must consider the different vertical modes separately. That part of the initial values that excites the external mode will behave like the barotropic case. For the higher vertical modes, however, we must also consider the horizontal scale, since it turns out that for large wavelength the wind tends to be adjusted to the height in middle and high latitudes.

ACKNOWLEDGMENTS

The author wishes to express his thanks to Prof. John B. Hovermale and to Dr. John A. Brown, Jr., and Dr. Joseph P. Gerrity, Jr., for reading the manuscript critically. He also wishes to thank Mr. Clifford H. Dey for permission to describe the results of his experiments and to Mrs. Zelda Licausi for typing the manuscript.

REFERENCES

Benwell, G. R. R., and Bretherton, F. P., "A Pressure Oscillation in a Ten-Level Atmospheric Model," *Quarterly Journal of the Royal Meteorological Society*, Vol. 94, No. 400, Apr. **1968**, pp. 123–131.

Blumen, William, "On Nonlinear Geostrophic Adjustment," *Journal of the Atmospheric Sciences*, Vol. 24, No. 4, July **1967**, pp. 325–332.

Blumen, William, and Washington, Warren M., "The Effect of Horizontal Shear Flow on Geostrophic Adjustment in a Barotropic Fluid," *Tellus*, Vol. 21, No. 2, **1969**, pp. 167–176.

Bolin, Bert, "The Adjustment of a Non-Balanced Velocity Field Towards Geostrophic Equilibrium in a Stratified Fluid," *Tellus*, Vol. 5, No. 3, Aug. **1953**, pp. 373–385.

Cahn, Albert, Jr., "An Investigation of the Free Oscillations of a Simple Current System," *Journal of Meteorology*, Vol. 2, No. 2, June **1945**, pp. 113–119.

Dey, Clifford H., "Some Characteristics of the Adjustment Process in an Initialization Procedure Which Uses a Forecast Model," National Meteorological Center, Weather Bureau, ESSA, Washington, D.C., **1969**, 14 pp., (unpublished manuscript).

Fjørtoft, Ragnar, "Stability Properties of Large-Scale Atmospheric Disturbances," *Compendium of Meteorology*, American Meteorological Society, Boston, **1951**, 1334 pp., (see pp. 454–463).

Kurihara, Yoshio, "On the Use of Implicit and Iterative Methods for the Time Integration of the Wave Equation," *Monthly Weather Review*, Vol. 93, No. 1, Jan. **1965**, pp. 33–46.

Lindzen, R. S., Batten, S. E., and Kim, J. -W., "Oscillations in Atmospheres with Tops," *Monthly Weather Review*, Vol. 96, No. 3, Mar. **1968**, pp. 133–140.

Miyakoda, K., and Moyer, R. W., "A Method of Initialization for Dynamical Weather Forecasting," *Tellus*, Vol. 20, No. 1, **1968**, pp. 115–128.

Morse, P. M., and Feshbach, H., *Methods of Theoretical Physics*, 2 vols., McGraw-Hill Book Co., Inc., New York, **1953**, (see pp. 719–729).

Nitta, T., "Initialization and Analysis for the Primitive Equation Model," paper presented at the WMO/IUGG Symposium on Numerical Weather Prediction, Tokyo, Nov.26–Dec. 4, **1968**.

Nitta, Takashi, and Hovermale, John B., "On Analysis and Initialization for the Primitive Forecast Equations," *ESSA Technical Memorandum* WBTM-NMC 42, National Meteorological Center, Washington, D.C., Oct. **1967**, 38 pp.

Obukhov, A., "K voprosu o geostrofischeskom vetra," (On the Question of Geostrophic Wind), *Akademiia Nauk SSSR, Izvestiia Seriia geograficheskaia geofizicheskaia*, Vol. 13, No. 4, Moscow, **1949**, pp. 231–306.

Ogura, Yoshimitsu, and Charney, Jule G., "A Numerical Model of Thermal Convection in the Atmosphere," *Proceedings of the International Symposium on Numerical Weather Prediction, Tokyo, November 7–13, 1960*, The Meteorological Society of Japan, Tokyo, Mar. **1962**, pp. 431–451.

Phillips, Norman A., "On the Problem of Initial Data for the Primitive Equations," *Tellus*, Vol. 12, No. 2, May **1960**, pp. 121–126.

Rossby, Carl G., "On the Mutual Adjustment of Pressure and Velocity Distribution in Certain Simple Current Systems, II," *Journal of Marine Research*, Vol. 1, **1938**, pp. 239–263.

Washington, Warren M., "A Note on the Adjustment Towards Geostrophic Equilibrium in a Simple Fluid System," *Tellus*, Vol. 16, No. 4, Nov. **1964**, pp. 530–534.

[Received August 29, 1969; revised October 8, 1969]